BioNanoScience (2023) 13:1933–1943
https://doi.org/10.1007/s12668-023-01218-7

Unlocking the Antimicrobial, Antifungal, and Anticancer Power of Chitosan-Stabilized Silver Nanoparticles

Ann Maria C G[1] · Ananya S Agnihotri[1] · Tazeen Fatima[2] · Saif Hameed[2] · Krishnamoorthy G[3] · Nidhin M[1]

Accepted: 7 October 2023 / Published online: 27 October 2023

Abstract
Silver nanoparticles (AgNPs) have become a research focus due to its antimicrobial, anticancer applications and cost-effective properties. In this study the effectiveness of green synthesis of NPs using biological macromolecule chitosan which is acting as a reducing cum stabilizing agent is carried out. An in-depth analysis of the synthesized AgNPs was conducted using a variety of sophisticated characterization techniques such as UV-visible spectroscopy, particle size analysis, zeta potential measurements, transmission electron microscopy (TEM), photoluminescence, and Fourier transform infrared (FTIR) spectroscopy. The antimicrobial activity of the formulated AgNPs were inspected against two human pathogenic strains. In the antimicrobial activity, the synthesized AgNPs exhibited a reduction in the growth of both the microbes. The minimum inhibitory concentration (MIC) of 1.22 μM was observed for both *Candida albicans* and *Mycobacterium smegmatis.* Consequently, AgNPs may be used as an opportunity for modern-day antibiotics to treat infections due to human pathogens. Antiproliferative analysis revealed that AgNPs showed antiproliferative characteristics against MDA-MB-231 cells compared to the control. Such AgNPs have an anticancer effect and are likely to be used as smart drug delivery mediators to treat late-stage cancer.

Keywords Green synthesis · Chitosan-stabilized silver nanoparticles · *Candida* · *Mycobacterium* · MDA-MB-231 cells

1 Introduction

Nanotechnology, the cynosure of research, is finding applications in almost all areas of human life [1]. Nanomaterials have unique properties on the nanoscale (1–100 nm) rather than in bulk, owing to their increased surface-to-volume ratio and surface area [2]. Nanomaterials are either produced by a top-down or bottom-up approach, where the latter method is preferred over others as one can synthesize the desired quality nanomaterials with customized shapes and properties by adjusting and optimizing the reaction conditions during nanoparticle synthesis [3]. Nanomaterial preparation involves nano-precursors, stabilizers, reducing agents, and capping agents for tailored morphology and applications [4]. The classic and traditional methods employed to formulate metal nanoparticles are chemical reduction [5], gamma irradiation [6], laser ablation, etc., involving hazardous chemicals that cause environmental pollution.

In contrast, green synthesis allows hassle-free preparation of nanomaterials with nontoxic reagents like plant extract, which is very cost-effective and abundant in nature [7, 8]. Green nanotechnology is popular with its different applications in the antimicrobial, antifungal, and anticancer studies [9]. Here, the biological macromolecules act as a reducing and stabilizing agent in synthesizing metal nanoparticles. Even though physical, chemical, and biological pathway of synthesis is prevailed, the most advantageous is the latter due to its rapid preparation, biocompatibility, use of nontoxic reagents and so on [10, 11].

Silver nanoparticles are used extensively compared to other metal nanoparticles because to their low cost and better properties [12–14]. Many studies use plant extract and biopolymers to synthesize silver nanoparticles [8, 15]. Chitosan is a biopolymer hydrophilic polysaccharide used as a template for synthesizing nanoparticles. Also, it acts as a

✉ Nidhin M
nidhin.m@christuniversity.in

[1] Department of Chemistry, CHRIST (Deemed to be University), Bengaluru 560029, India

[2] Amity Institute of Biotechnology, Amity University Haryana, Amity Education Valley, Gurugram 122413, India

[3] Muthayammal Centre for Advanced Research (MCAR) & Department of Biochemistry, Muthayammal College of Arts and Science (Affiliated to Periyar University, Salem), Rasipuram, Namakkal District, Tamil Nadu 637408, India

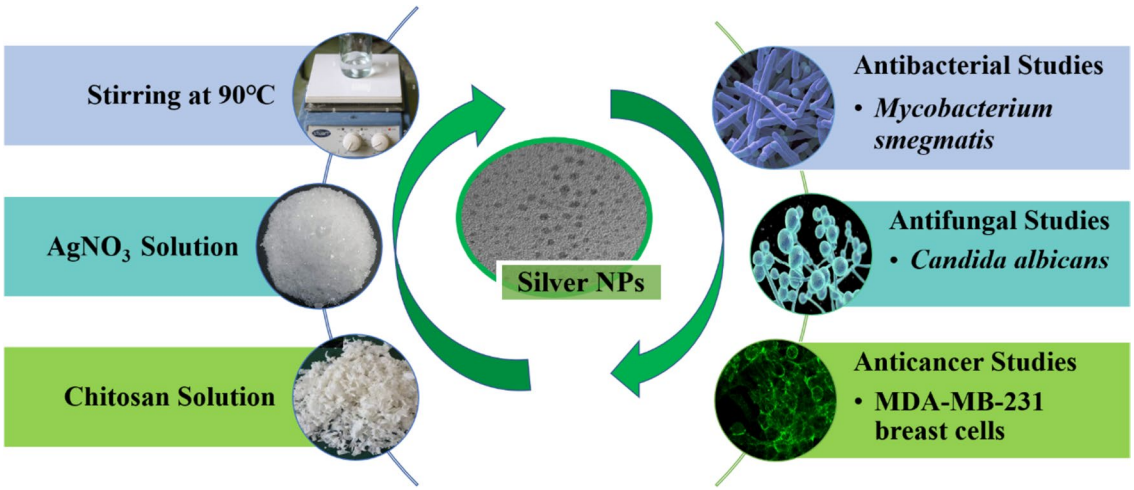

Scheme 1 A schematic view of the environmentally friendly production of chitosan-stabilized AgNPs and its applications in antibacterial, antifungal, and anticancer studies

stabilizing agent, reducing agent, and capping agent in different systems accordingly [16, 17]. Originating from chitin, chitosan is the second-most common biopolymer in world. Using chitosan for silver reduction is possible because Ag^+ ions are effortlessly reducible by the electrons (lone pair) in N and O atoms in chitosan, facilitating the complex formation and reduction of silver ions. Thus, the reduction was possible in this study due to the intrinsic property of chitosan, which does not employ any external chemical-reducing agent. An overview of the study is included as Scheme 1, consisting of the synthesis route and application of the formulated NPs. Even though many studies are reported on the synthesis of silver nanoparticles, the presence of chitosan as the reducing and stabilizing agent plays a vital role in the synthesis of AgNPs. The smaller size and spherical shape of the AgNPs are very useful for biological activity.

Even though AgNPs find applications in all fields, the significant contribution of publications is from biomedical applications [18, 19]. From ancient times, silver nanoparticles were used for treatment [20, 21]. In the present scenario, using silver nanoparticles for antibacterial applications is a boon where antibiotics and overdosing of antibiotics result in drug resistance and many have side effects on the human body. The excessive application of antimicrobial drugs has generated a problem branded as multidrug resistance (MDR), in which bacterial and fungal pathogens acquire resistance to multiple drugs. [22]. It is imperative to uncover new drugs to fight human pathogens [23]. *Mycobacterium tuberculosis* is a deadly pathogen that causes fatalities globally [24]. Hospital-acquired infections, primarily fungal infections from *Candida albicans,* are the fourth most common cause of mortality [25]. AgNPs have been investigated for their potential anticancer qualities due to the potential of silver ions or radical species to cause cellular damage and death [26]. They demonstrate innate anticancer properties and can be utilized as carriers of anticancer drugs, leading to a dual therapeutic healing. Through this research, we aim to explore the biomedical applications of chitosan-stabilized colloidal silver nanoparticles. The synthesized silver nanoparticle was characterized and assessed their MIC using two different human pathogens like, *Candida albicans* and *Mycobacterium*, and the anticancer potential of the synthesized AgNPs was also analyzed using MDA-MB-231 cells in this study.

2 Experimental

2.1 Chemicals and Reagents

Dulbecco's Modified Eagle's Medium, penicillin-G, phosphate buffered saline, streptomycin, L-glutamine, 3-(4,5 dimethylthiozol-2-yl)-2,5-diphenyltetrazoliumbromide, 2′7′diacetyl dichloro fluorescein, sodium dodecyl sulfate, glacial acetic acid, trypan blue, trypsin-EDTA, ethylene diamine tetra acetic acid, ethidium bromide, rhodamine-123, acridine orange, ethanol, dimethyl sulfoxide (DMSO), triton X-100, silver nitrate ($AgNO_3$), chitosan with a deacetylation degree > 75%, and bovine serum albumin were acquired from Sigma Aldrich Chemicals Pvt. Ltd (India). Double distilled (DD) water was used for all aqueous solution preparations. All other chemical compounds used had been of analytical quality, bought from Hi Media Laboratories Pvt. Ltd., India. Breast cancer (MDA-MB-231) cell lines were obtained from the Cell repository of the National Centre for Cell Sciences (NCCS), Pune, India.

2.2 Synthesis of Chitosan-Stabilized AgNPs

The synthesis of AgNPs were done in the same way as in our previous paper [27]. Chitosan solution 0.5 % (w/v) is first made using 2% glacial acetic acid through stirring for 30 min and filtered to remove all the impurities. To this solution, add 0.01 M $AgNO_3$ solution, and stir the solution for 30 min at 90 degrees Celsius. The color change of the solution was from colorless to light yellow and finally to a light brown hue after 30 min. Once cooled, the colloidal AgNPs have a brown hue.

2.3 Characterization techniques

In a Japanese Shimadzu (UV 2500) UV-visible spectrophotometer, absorption peak was observed for the synthesized AgNPs in the range of 300 to 700 nm. Dynamic light scattering (DLS) methods were utilized to assess the particle size distribution and the average hydrodynamic diameter using a Zetasizer NanoZS ZS ZEN 3600 equipment from Malvern Instruments Ltd. Based on the electrophoretic mobility measurement method of laser doppler velocimetry, zeta potential analysis were performed using the same device, the Zetasizer Nano ZS ZEN 3600. (LDV). Additionally, utilizing a Tensor 37, samples were examined using Fourier-transformed infrared spectroscopy (FTIR) (Bruker, Munich, Germany). A measuring range of 4000–400 cm^{-1} was used to record the data. With a LaB_6 source attached, the JEOL 2100 was used for TEM studies. The PL measurements were made with a Shimadzu RF-5301 PC.

2.4 Anticandidal Activity

2.4.1 Fungal Strains and Culture Conditions

SC5134 was the *C. albicans* reference strain used in this investigation. YEPD broth, which contains 2% (w/v) peptone, 2% (w/v) dextrose, and 1% (w/v) yeast extract, was used to cultivate C. albicans. Agar was added 2% (w/v) (in the media) for agar plates. At − 80°C, the Candida strain was kept in a 30% (v/v) glycerol stock. To confirm the revival of the strains, freshly revived cells (on YEPD broth) are shifted before each experiment to an agar plate.

2.4.2 Minimum Inhibitory Concentration (MIC) and Spot Assay

Method M27-A3 of CLSI, the Clinical and Laboratory Standards Institute, was used to determine the MIC [28]. Following the inclusion of the AgNPs with the remaining media, an aliquot of 100 μl has been poured to the wells of 96-well plate and serially diluted. In order to test for anticandidal activity, a stock solution of 100 mM concentration was made and diluted to a range of concentrations ranging from 78.12 to 0.15 μM. After 48 h at 30 °C, the OD_{600} of the 100 μl of cell suspension (in normal saline to an OD_{600} of 0.1) in each well of the plate was measured. The concentration at which at least 90% of the growth was inhibited was referred to as the MIC90. Spot assays were carried out using a technique that has been previously described [29]. For the spot assay, 5 μl yeast culture (fivefold serial dilutions) were spotted in both the absence (control) and presence of the AgNPs onto YEPD plates, with each dilution having cells suspended in ordinary saline to an OD_{600} nm of 0.1. After 48 h at 30 °C, the growth difference was measured.

2.5 Antimycobacterial Activity

2.5.1 Bacterial Strain and Culture Conditions

In standard flasks of 100 mL (Schott Duran) containing Middlebrook 7H9 (BD Biosciences) broth supplemented with 0.05% tween-80, 10% ADC, and 0.2% glycerol, *Mycobacterium* cells were cultivated until the exponential phase was attained. Stock cultures of cells (log phase) were kept in 30% glycerol and kept at − 80 °C. *M. smegmatis* mc2155 is the bacterial strain used in the present study.

2.5.2 MIC and Spot Assay

As described in the literature [28–30], the minimum inhibitory concentration (MIC) testing was conducted. Each well on the 96-well plate received approximately 100 μl of Middlebrook 7 H9 broth supplemented with glycerol 0.05% (v/v), Tween80, and OADC enrichment 0.5% (v/v). A 100 μl of cell suspension (equal to the McFarland standard 0.5) was put into each well of the plate, and then the drug was added together with the residual media, and finally, it was serially diluted in the ratio 1:2. The $O.D_{600}$ in a microplate reader was used to determine the MIC values (Elisa Reader). In the spot experiment, Middlebrook 7H10 agar plates were spotted with 5 µL of fivefold serial dilutions of each *M. smegmatis* culture (each with cells suspended in normal saline to an OD_{600} nm of 0.1) in both the absence (control) and presence of the AgNPs. After incubation at 37 °C for 48 h, growth difference was assessed in both trials.

2.6 Anticancer Activity

The cell line was sustained in Dulbecco's Modified Eagle Media (DMEM), which was enhanced with 10% fetal bovine serum (FBS). To prevent contamination through bacteria, streptomycin (100 μg/ml) and penicillin (100 U/ml) was put to the medium. The medium containing the cell lines was kept at 37 °C in a moist atmosphere with 5% CO_2.

2.6.1 MTT Assay

The Mosmann method [31] was used to assess the cytotoxicity of colloidal AgNPs stabilized by chitosan on MDA-MB-231 cells. The cells were grown with the dispersion of free colloidal AgNPs (negative control), colloidal AgNPs (positive control), and chitosan-stabilized colloidal AgNPs in a 96-well culture plate. The mitochondrial dehydrogenase of live cells reduces the yellow 3-4,5dimethylthiozol-2-Yl)-2,5diphenyltetrazoliumbromide (MTT), producing a detectable purple formation product. The NAD(P)H-dependent reductase found in viable cells transforms the MTT reagent into formazan, an ingredient with a deep purple hue. Following the solubilizing solution's dissolution of the formazan crystals, a plate reader measures absorbance between 500 and 600 nm. A 10 mL of PBS was utilized to dissolve 50 mg of MTT dye. It was filtered using 0.45 micro filters after 1 min of vortexing. Since MTT was light-sensitive, the bottle was covered in aluminum foil to block off the light. At 4 °C, the preparation was kept. MDA-MB-231 viable cells were extracted for the cell viability assay, counted using a hemocytometer, and diluted in DMEM media to a density of 1104 cells/ml before being planted in 96-well plates and cultured for 1 day to promote attachment. Following treatment with colloidal AgNPs (control) and various doses of chitosan-stabilized colloidal AgNPs (10–12.5 μg/ml), MDA-MB-231 cells were added to each well. For 24 h, MDA-MB-231 cells were incubated at 37 °C in an incubator with humidified 95% air and 5% CO_2. The chitosan-stabilized colloidal AgNPs containing cells were incubated for 4 h at 37 °C after washing with fresh culture media and adding the MTT (5 mg/ml in PBS) dye to each well. The cell viability was evaluated by absorbance at 540 nm using a multi-well plate reader, and the purple precipitated formazan was dissolved in 100 μL of concentrated DMSO. The percentage of stable cells compared to the control was used to express the results.

$$\text{Inhibitory of cell proliferation (\%)} = \frac{\text{Mean absorbance of the control} - \text{Mean absorbance of the sample}}{\text{Mean absorbance of the control}} \times 100$$

Each experiment was run in duplicate at least three times.

3 Results and Discussion

3.1 Characterizations of the synthesized AgNPs

An extensive characterization of the synthesized AgNPs were conducted using various characterization techniques like UV-Visible spectroscopy, photoluminescence spectroscopy, dynamic light scattering techniques such as particle size distribution and zeta potential measurements, TEM and FT-IR spectroscopy.

3.1.1 UV-Visible Spectroscopy

UV-Visible spectroscopy is the primary confirmation method for the formation of AgNPs. Visual observation revealed that the color of the solution had changed from colorless to light yellow, then to yellowish-brown, which supported the synthesis of AgNPs. The activation of $AgNO_3$'s surface plasmon resonance (SPR) causes the yellowish-brown color to become more intense. Kinetic measurements were made of the solution's light absorption pattern between 300 and 700 nm. In an aqueous solution, size- and shape-controlled NPs could be examined using UV-vis spectroscopy. AgNPs from crab shell waste showed a distinctive absorbance peak observed at 422 nm in the spectrum (Fig. 1). The fact that this peak could be attributed to an SPR of metal NPs and that it did not broaden suggested that the particles were monodispersed. The peak characteristic to bulk Ag at 320 nm in the UV-Vis spectra typically represents the 4d to 5sp inter-band transitions in this material. However, the silver nanoparticles' dispersion exhibits a redshift, and the peak at 320 nm changed to 422 nm, matching the dipole resonance of spherical silver nanoparticles, further supported by TEM images.

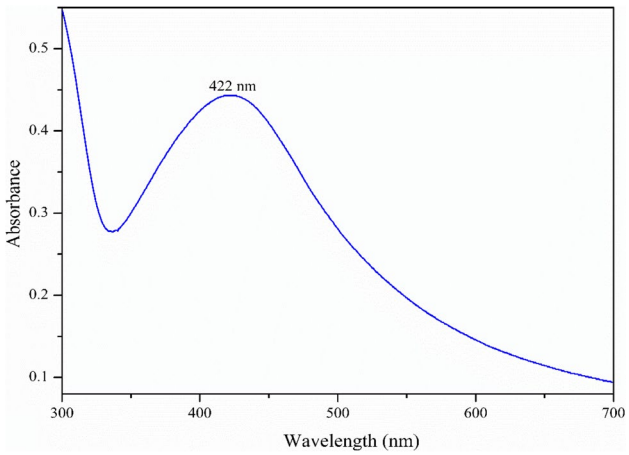

Fig. 1 UV visible spectra of chitosan-stabilized colloidal silver nanoparticle

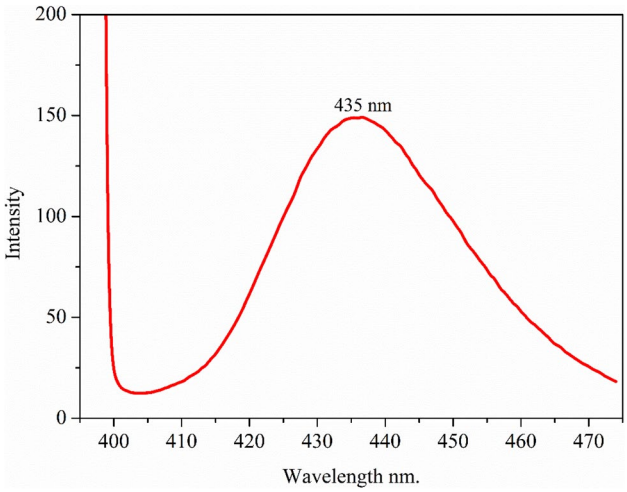

Fig. 2 Fluorescence emission of chitosan-stabilized silver nanoparticle at 435 nm

3.1.2 Photoluminescence Spectroscopy

The synthesized nanomaterials exhibit photoluminescence which is a further plus point to the study (Fig. 2). When the size of metal particles is decreased to 2 nm, the energy bands are replaced by discrete energy levels, and this induces electronic transitions with interaction with electromagnetic waves resulting in absorbance and fluorescence.

The size and shape of the nanoparticles influence the absorption and emission spectra. Strong fluorescence emission was observed for the synthesized spherical-shaped silver nanoparticles with $\lambda_{em} = 435$ nm ($\lambda_{ex} = 422$ nm). The observed fluorescence can be attributed to the recombination of sp electrons with holes in the d band. The synthesized AgNPs can be further used for optical sensor applications.

3.1.3 Dynamic Light Scattering (DLS)

Dynamic light scattering was used to study the particle size distribution of the synthesized silver nanoparticles' using chitosan as template. The hydrodynamic diameter of the synthesized AgNPs was observed to be 6.266 nm (Fig. 3), and the smaller size of the obtained NPs can be attributed to the occurrence of the chitosan template. The value of the hydrodynamic diameter of the synthesized nanoparticles is more or less similar to the results obtained from TEM (2.5 nm).

The zeta potential measurement of the sample was carried out to comprehend the stability of the synthesized AgNPs. The measurement gives an idea about the surface charge around the nanoparticle and its colloidal stability. The zeta potential of the synthesized nanoparticles was observed to be − 2.64 mV, and the negative charge shows the potential of these silver nanoparticles in biological applications (Fig. 4). The biological entity in chitosan provides a negative charge to the nanoparticle, which helps stabilize nanoparticles and ultimately prevents agglomeration.

3.1.4 Transmission Electron Microscopy (TEM)

The transmission electron microscopy is employed for detecting the morphology of the synthesized AgNPs. Figure 5 shows the TEM images of the synthesized chitosan-stabilized AgNPs. The TEM images clearly show the spherical shape of the synthesized silver nanonanoparticles with uniform particle size distribution. In the TEM images, the

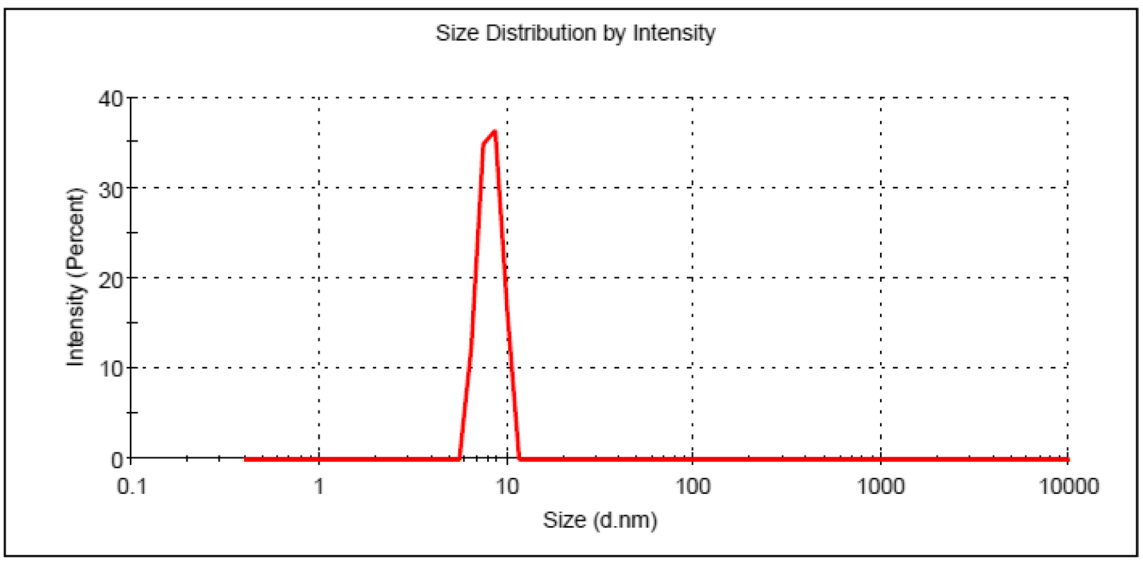

Fig. 3 The particle size distribution by DLS where the Z-average diameter was 6.266 nm and a PDI of 0.364

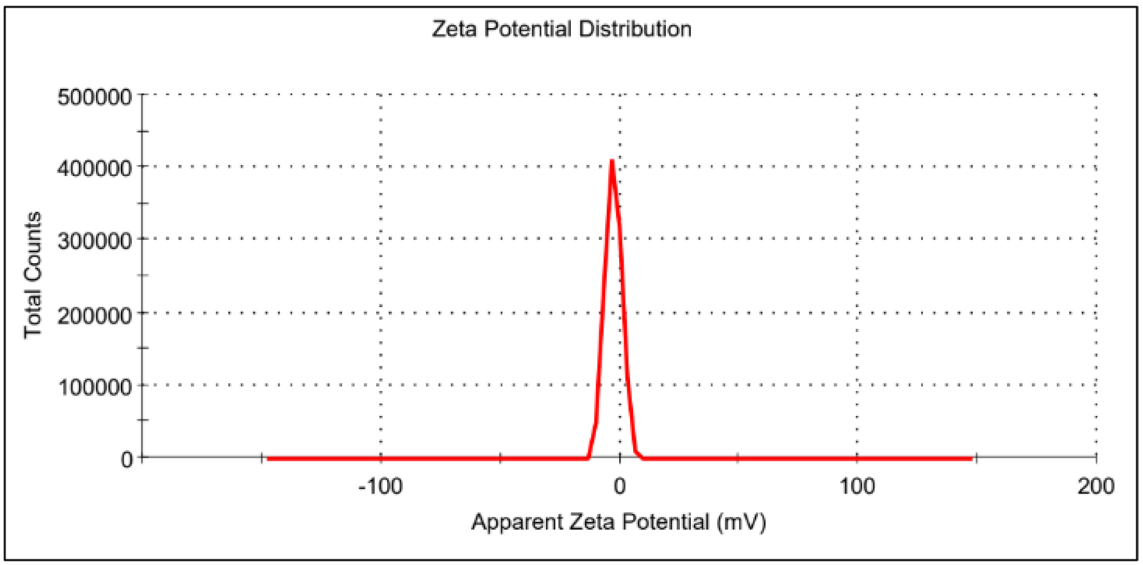

Fig. 4 Zeta potential distribution of chitosan-mediated biogenic silver nanoparticles with an apparent zeta potential of − 2.64 mV

bright color corresponds to chitosan template matrix, and dark spots refer to the AgNPs embedded in the chitosan matrix. A statistical particle distribution curve is included, which is obtained using Image J software. The average particle size distribution) of the formulated silver NPs was observed to be 2.5 nm. The SAED (selected area electron diffraction) is used to identify whether a material is monocrystalline or polycrystalline in nature. The concentric ring-like diffraction pattern and some bright spots in SAED images indicate that the particles are polycrystalline in nature. The interplanar distance d (1/r where r is the radius of the concentric circle) value was found to be 0.282 nm and 0.1452 nm suggesting the FCC crystal lattice of the AgNPs.

3.1.5 FTIR Analysis

In our study, we used FTIR analysis to determine functional groups in the chitosan template and the synthesized silver nanoparticles. Figure 6a denotes the FTIR spectrum of the chitosan template, and Fig. 6b represents the FTIR spectra of the synthesized silver nanoparticles. Figure 6a depicts two distinct bands in the pure chitosan spectrum: one at 3311 cm^{-1}, matching to the -OH stretching, and the other at 1640 cm^{-1}, matching to the -$CONH_2$ group. The -OH stretching band is at 3307 cm^{-1} in Fig. 6b, while the band corresponding to the -$CONH_2$ group is shown at 1638 cm^{-1}. The band at 3300 cm^{-1} in the pure chitosan spectra is expanded and slightly shifted to 3307 cm^{-1} in Fig. 6b. This shift may be due to the interaction of the chitosan template with the AgNPs. The amino groups of chitosan are displaced to a lower wavelength of 1638 cm^{-1}, where the AgNPs' minor changes in the IR spectrum of the particles occur. This demonstrates that the interaction between the primary -NH_2 and -OH groups found in the template and the nanoparticles' surface causes AgNPs to be stabilized by chitosan.

3.1.6 Optimization of Experimental Conditions

The optimization of experimental conditions required for the preparation of silver nanoparticles were carried out. The first parameter to be optimized were the weight percentage of the chitosan solution used to prepare the nanoparticle. The viscosity of the chitosan solution increased with increasing weight percentage. The studies were conducted with a lower weight percentage of about 0.5 wt% of chitosan solution with an optimal volume of acetic acid as 2 ml. The parameter to be considered were the concentration of silver nitrate, the precursor for synthesizing silver nanoparticles. The optimum concentration for the synthesis of nanoparticles were found to be 0.01 M for $AgNO_3$, giving a smaller particle size and low PDI value. The PDI value reflects the uniformity of the synthesized AgNPs, and it is in the range of 0.01 to 0.7 for a monodisperse system, and values more than 0.7 correspond to the polydisperse nature of the synthesized nanoparticles. The comparison of different optimization conditions such as weight % of chitosan solution, the concentration of the $AgNO_3$, volume of glacial acetic acid, hydrodynamic diameter, and PDI of the formulation of AgNPs are summarized in Table 1.

The biological activity of these inorganic nanoparticles were depends upon certain factors like size distribution, surface charge, surface chemistry, and morphology [32, 33]. Considering these factors, the synthesized

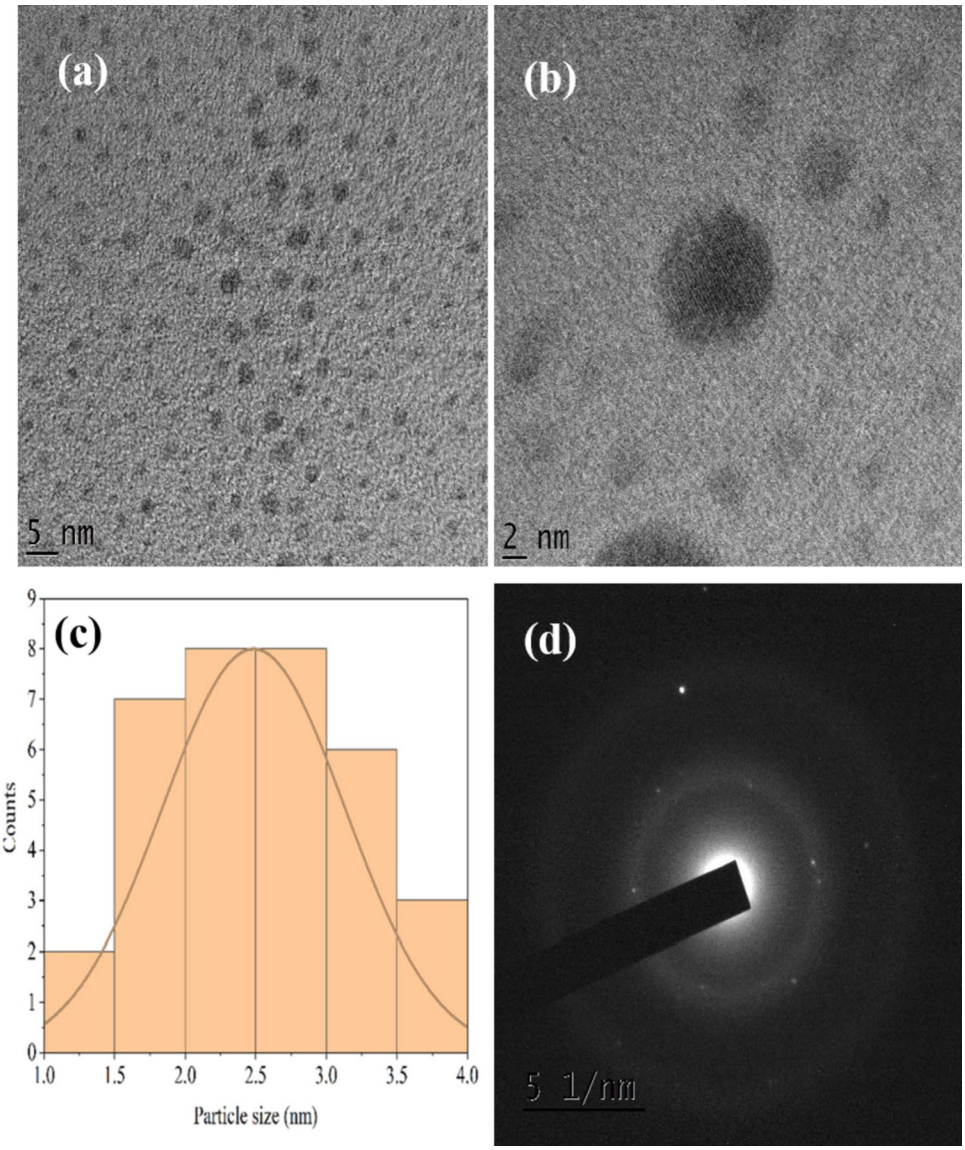

Fig. 5 TEM images (**a**, **b**) of the synthesized AgNPs using chitosan as a template with particle size in the range of **a** 5 nm, **b** 2 nm, **c** particle size distribution, and **d** SAED pattern of the formulated AgNPs

chitosan-stabilized silver nanoparticles were taken for biological applications such as antifungal, antibacterial, and cell viability studies and anticancer activities.

3.2 Antifungal and Antibacterial studies

In order to investigate the potential of AgNP as an antimicrobial agent, two independent procedures were employed to evaluate the antimicrobial efficacy of AgNP on two diverse human pathogens, *Candida albicans* and *Mycobacterium*. Primarily, MIC of AgNP was estimated by broth microdilution method, and it was found that 1.22 μM of AgNP was sufficient to inhibit both *Candida albicans* (Fig. 7) and *Mycobacterium smegmatis*, a widely used nonpathogenic surrogate for MTB (Fig. 8) respectively. The spot assay reconfirmed the earlier results, showing that 1.22 μM concentration of AgNP was effective in inhibiting both microbes.. In order to combat the issue of drug-resistance in these two human pathogens, combinatorial therapy using nanoparticles could be a viable alternative to existing drugs, augmenting their effectiveness.

3.3 Cell Viability Analysis

The chitosan-stabilized colloidal AgNPs were used as transporters for drug delivery applications, by evaluating their biocompatibility for in vivo applications. To prevent cellular death due to competition for space, the cell viability tests were conducted for a three day period. Figure 9 depicts the cell viability of various concentrations of chitosan-stabilized colloidal AgNPs treated samples. To make easier comparisons with colloidal AgNPs that have been stabilized

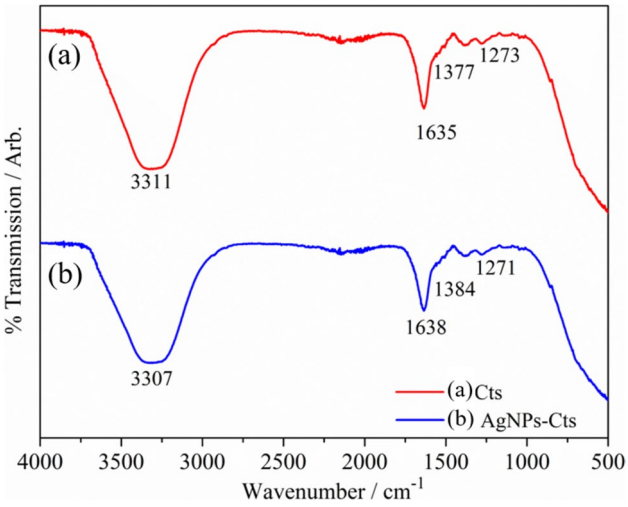

Fig. 6 **a** FTIR Spectra of chitosan template and **b** chitosan-stabilized silver nanoparticles

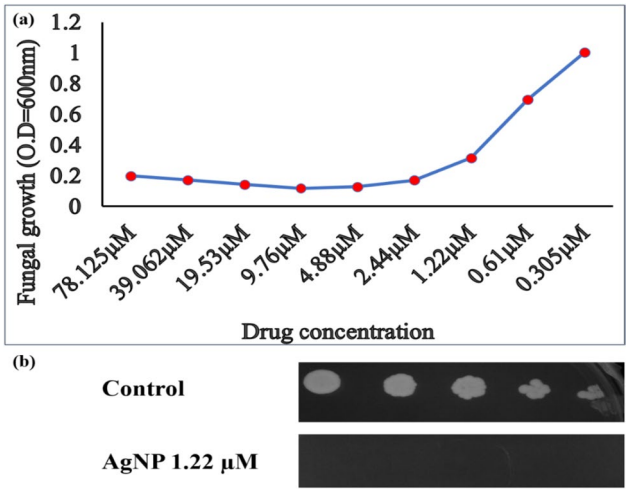

Fig. 7 Antifungal activity of AgNP against *C. albicans*. **a** Broth microdilution assay depicting MIC. **b** Spot assay validating the MIC

by chitosan, the control was treated as 100% growth at any concentration. Remarkably, the number of cells grew over time. After 1 day, almost 95% of viable cells rose to 112.5% after three days. According to the findings, cell growth is unaffected and equivalent to control cells.

3.3.1 Anticancer Activity

Photomicrograph (10 ×) shows the morphological alterations in MDA-MB-231 cells brought on by treatment with chitosan-stabilized colloidal AgNPs (10 and 12.5 μg/ml for 24 h), as related to control, including detachment, membrane blebbing, shrinkage, and deformed shape profile. The photos of the control cells, which had normal, intact cell morphology, were taken. As a result, the generated AgNPs have an

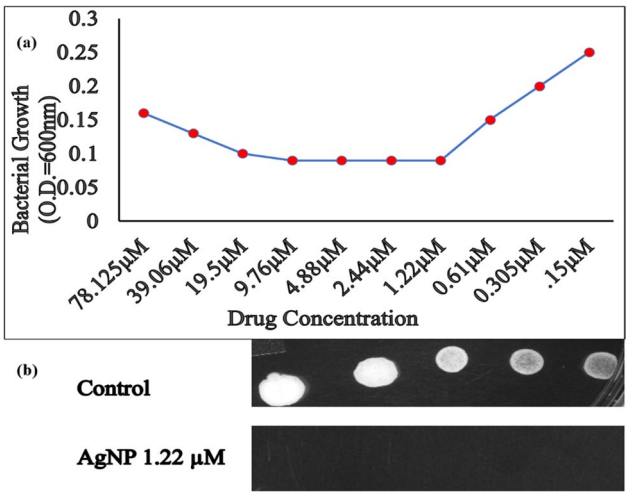

Fig. 8 Antibacterial activity of AgNP against *M. smegmatis*. **a** Broth microdilution assay depicting MIC. **b** Spot assay validating the MIC

Table 1 Comparison of different optimization parameters involved in synthesizing silver nanoparticles

Sample number	Weight % of chitosan solution	Concentration of $AgNO_3$ (M)	Volume of glacial acetic acid (ml)	Hydrodynamic diameter (nm)	Poly Dispersive Index (PDI)
1	0.5	0.01	2	6.266	0.364
2	0.5	0.1	2	19.18	0.409
3	1	0.001	10	6.603	0.572
4	1	0.01	20	19.89	0.393
5	1	0.02	10	105.5	0.473
6	1	0.1	2	11.39	0.355
7	1	0.1	1	156.9	0.472
8	1	0.5	2	146.1	0.137
9	2	0.01	10	150.5	0.104
10	3	0.01	10	64	0.362

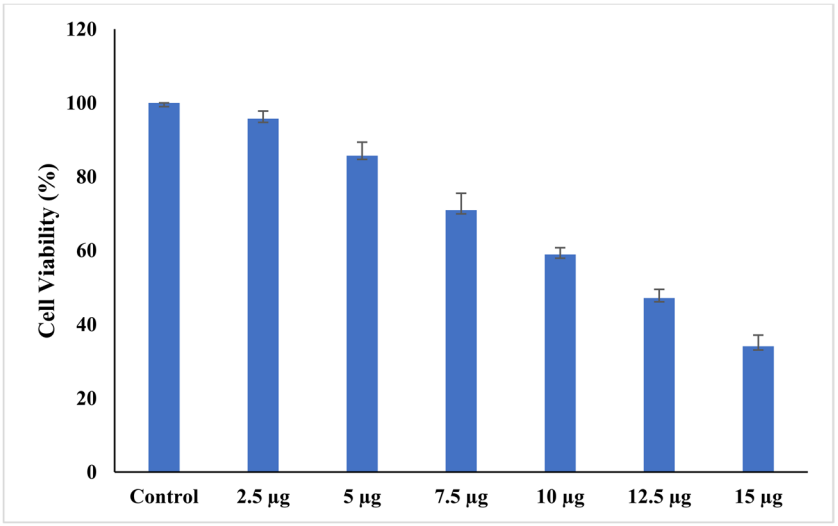

Fig. 9 Cell viability of control and chitosan-stabilized colloidal AgNPs treated cells for 24 h

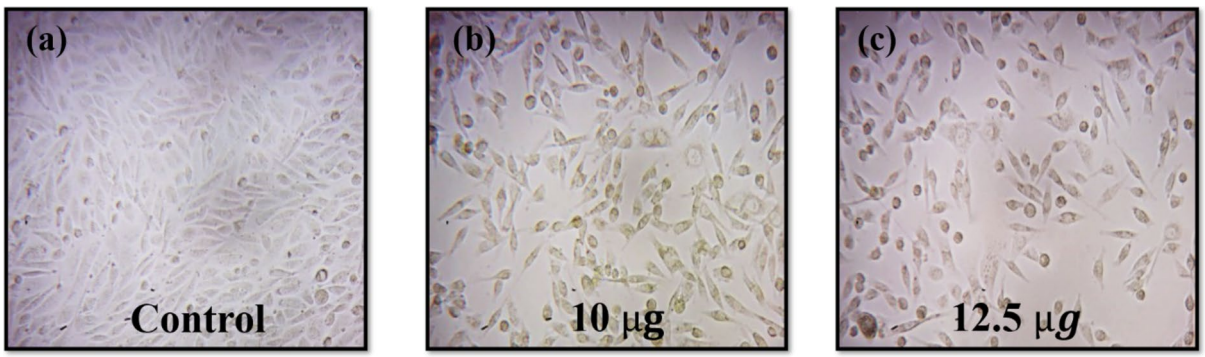

Fig. 10 Morphological changes in **a** control and **b** chitosan-stabilized colloidal AgNPs and **c** treated MDA-MB-231 cells for 72 h

effective potent cytotoxic effect on MDA-MB-231 cells than on other types of cell lines (Fig. 10).

4 Conclusion

In this research work, we have synthesized AgNPs utilizing chitosan as the bio template. The synthesis pathway adheres to nontoxic chemicals, simple preparation steps, and environment-friendly applications. The formulated AgNPs' size and morphology were examined using various characterization techniques, and it was discovered that they were small and very stable. Furthermore, the nanoparticles were taken for various antibacterial, antifungal, and anticancer studies. The MIC of the chitosan-stabilized AgNPs against *Candida albicans* and *Mycobacterium smegmatis* at 1.22 μM predicts the efficiency of these nanoparticles for various therapeutic and clinical applications. Colloidal AgNPs stabilized by chitosan exhibited in vitro antitumor efficacy against breast cancer cell lines (MDA-MB-231). Besides the pharmaceutical, food, and cosmetic industries, AgNPs can be utilized successfully in medicine due to their improved antibacterial, antifungal, and anticancer activities.

Author Contribution A. M. C. G.: conceptualization, investigation, methodology, writing-original draft. A. S. A.: investigation, data curation, writing-original draft. T. F.: methodology, data curation, writing-original draft. S. H.: investigation, formal analysis, writing-original draft. K. G. : methodology, formal analysis, writing-original draft. N. M.: writing-original draft, visualization, review and editing, supervision.

Funding The authors are grateful to Vision Group on Science and Technology, (VGST/RGS-F/GRD-922/2019-20/2020-21/198) for arranging the financial support for this research work.

Data Availability Not applicable.

Declarations

Ethical Approval Not applicable.

Competing Interests The authors declare no competing interests.

References

1. Mostafavi, E., Zarepour, A., Barabadi, H., Zarrabi, A., Truong, L. B., & Medina-cruz, D. (2022). Antineoplastic activity of biogenic silver and gold nanoparticles to combat leukemia: Beginning a new era in cancer theragnostic. *Biotechnology Reports, 34*, e00714. https://doi.org/10.1016/j.btre.2022.e00714
2. Bayda, S., Adeel, M., Tuccinardi, T., Cordani, M., & Rizzolio, F. (2020). The history of nanoscience and nanotechnology: From chemical-physical applications to nanomedicine. *Molecules, 25*(1), 1–15. https://doi.org/10.3390/molecules25010112
3. Geonmonond, R. S., Da Silva, A. G. M., & Camargo, P. H. C. (2018). Controlled synthesis of noble metal nanomaterials: Motivation, principles, and opportunities in nanocatalysis. *Anais da Academia Brasileira de Ciências, 90*(1), 719–744. https://doi.org/10.1590/0001-3765201820170561
4. Ali, S., Sharma, A. S., Ahmad, W., Zareef, M., Hassan, M. M., Viswadevarayalu, A., et al. (2021). Noble metals based bimetallic and trimetallic nanoparticles: Controlled synthesis, antimicrobial and anticancer applications. *Critical Reviews in Analytical Chemistry, 51*(5), 454–481. https://doi.org/10.1080/10408347.2020.1743964
5. Quintero-Quiroz, C., Acevedo, N., Zapata-Giraldo, J., Botero, L. E., Quintero, J., Zárate-Trivinõ, D., et al. (2019). Optimization of silver nanoparticle synthesis by chemical reduction and evaluation of its antimicrobial and toxic activity. *Biomaterials Research, 23*(1), 1–15. https://doi.org/10.1186/s40824-019-0173-y
6. Dhayagude, A. C., Das, A., Joshi, S. S., & Kapoor, S. (2018). γ-Radiation induced synthesis of silver nanoparticles in aqueous poly (N-vinylpyrrolidone) solution. *Colloids and Surfaces A: Physicochemical and Engineering Aspects, 556*, 148–156. https://doi.org/10.1016/j.colsurfa.2018.08.028
7. Gour, A., & Jain, N. K. (2019). Advances in green synthesis of nanoparticles. *Artificial Cells, Nanomedicine and Biotechnology, 47*(1), 844–851. https://doi.org/10.1080/21691401.2019.1577878
8. Meera, V. P. A. S., & Maria, C. G. A. (2022). Green synthesis of nanoparticles from biodegradable waste extracts and their applications : A critical review. *Nanotechnology for. Environmental Engineering*, (0123456789). https://doi.org/10.1007/s41204-022-00276-8
9. Barabadi, H., Mobaraki, K., Jounaki, K., & Sadeghian-abadi, S. (2023). Heliyon Exploring the biological application of penicillium fimorum- derived silver nanoparticles: In vitro physicochemical , antifungal , biofilm inhibitory , antioxidant , anticoagulant , and thrombolytic performance. *Heliyon, 9*(6), e16853. https://doi.org/10.1016/j.heliyon.2023.e16853
10. Vahidi, H., Kobarfard, F., Alizadeh, A., Saravanan, M., & Barabadi, H. (2020). Green nanotechnology-based tellurium nanoparticles: Exploration of their antioxidant, antibacterial, antifungal and cytotoxic potentials against cancerous and normal cells compared to potassium tellurite. *Inorganic Chemistry Communications*, 108385. https://doi.org/10.1016/j.inoche.2020.108385
11. Cruz, D. M., Mostafavi, E., Vernet-crua, A., Barabadi, H., Shah, V., & Jorge, L. (2020). Green nanotechnology-based zinc oxide (ZnO) nanomaterials for biomedical applications: a review. *JPhys Materials, 3*(3), 0–25. https://doi.org/10.1088/2515-7639/ab8186
12. Lee, S. H., & Jun, B. H. (2019). Silver nanoparticles: Synthesis and application for nanomedicine. *International Journal of Molecular Sciences, 20*(4). https://doi.org/10.3390/ijms20040865
13. Crisan, C. M., Mocan, T., Manolea, M., Lasca, L. I., Tăbăran, F. A., & Mocan, L. (2021). Review on silver nanoparticles as a novel class of antibacterial solutions. *Applied Sciences (Switzerland), 11*(3), 1–18. https://doi.org/10.3390/app11031120
14. Akhil, T., Bhavana, V., Ann Maria, C. G., & Nidhin, M. (2023). Role of biosynthesized silver nanoparticles in environmental remediation: A review. *Nanotechnology for. Environmental Engineering*, 0123456789. https://doi.org/10.1007/s41204-023-00324-x
15. Alavi, M., & Rai, M. (2019). Recent progress in nanoformulations of silver nanoparticles with cellulose, chitosan, and alginic acid biopolymers for antibacterial applications. *Applied Microbiology and Biotechnology, 103*(21–22), 8669–8676. https://doi.org/10.1007/s00253-019-10126-4
16. Restrepo, C. V., & Villa, C. C. (2021). Synthesis of silver nanoparticles, influence of capping agents, and dependence on size and shape: A review. *Environmental Nanotechnology, Monitoring and Management, 15*, 100428. https://doi.org/10.1016/j.enmm.2021.100428
17. Franconetti, A., Carnerero, J. M., Prado-Gotor, R., Cabrera-Escribano, F., & Jaime, C. (2019). Chitosan as a capping agent: Insights on the stabilization of gold nanoparticles. *Carbohydrate Polymers, 207*, 806–814. https://doi.org/10.1016/j.carbpol.2018.12.046
18. Abdulsahib, S. S. (2021). Synthesis, characterization and biomedical applications of silver nanoparticles. *Biomedicine (India), 41*, 458–464. https://doi.org/10.51248/.v41i2.1058
19. Burdușel, A. C., Gherasim, O., Grumezescu, A. M., Mogoantă, L., Ficai, A., & Andronescu, E. (2018). Biomedical applications of silver nanoparticles: An up-to-date overview. *Nanomaterials, 8*(9), 1–25. https://doi.org/10.3390/nano8090681
20. Alexander, J. W. (2009). History of the medical use of silver. *Surgical Infections, 10*(3), 289–292. https://doi.org/10.1089/sur.2008.9941
21. Barillo, D. J., & Marx, D. E. (2014). Silver in medicine: A brief history BC 335 to present. *Burns, 40*(S1), S3–S8. https://doi.org/10.1016/j.burns.2014.09.009
22. Catalano, A., Iacopetta, D., Ceramella, J., Scumaci, D., Giuzio, F., Saturnino, C., et al. (2022). Multidrug resistance (MDR): A widespread phenomenon in pharmacological therapies. *Molecules, 27*(3), 1–18. https://doi.org/10.3390/molecules27030616
23. Ghuglot, R., Titus, W., Agnihotri, A. S., Krishnakumar, V., Krishnamoorthy, G., & Marimuthu, N. (2021). Stable copper nanoparticles as potential antibacterial agent against aquaculture pathogens and human fibroblast cell viability. *Biocatalysis and Agricultural. Biotechnology, 32*. https://doi.org/10.1016/j.bcab.2021.101932
24. Singh, R., Dwivedi, S. P., Gaharwar, U. S., Meena, R., Rajamani, P., & Prasad, T. (2020). Recent updates on drug resistance in Mycobacterium tuberculosis. *Journal of Applied Microbiology, 128*(6), 1547–1567. https://doi.org/10.1111/jam.14478
25. Carolus, H., Van Dyck, K., & Van Dijck, P. (2019). Candida albicans and Staphylococcus species: A threatening twosome. *Frontiers in Microbiology, 10*. https://doi.org/10.3389/fmicb.2019.02162
26. Gomes, H. I. O., Martins, C. S. M., & Prior, J. A. V. (2021). Silver nanoparticles as carriers of anticancer drugs for efficient target treatment of cancer cells. *Nanomaterials, 11*(4). https://doi.org/10.3390/nano11040964
27. Ann Maria, C. G., Agnihotri, A. S., Varghese, A., & Nidhin, M. (2023). Ion-imprinted chitosan-stabilized biogenic silver nanoparticles for the electrochemical detection of arsenic (iii) in water samples. *New Journal of Chemistry, 47*(11), 5179–5192. https://doi.org/10.1039/d2nj04804c
28. Hans, S., Fatima, Z., & Hameed, S. (2019). Magnesium deprivation affects cellular circuitry involved in drug resistance and virulence in Candida albicans. *Journal of Global Antimicrobial Resistance, 17*, 263–275. https://doi.org/10.1016/j.jgar.2019.01.011

29. Nidhin, M., Saneha, D., Hans, S., Varghese, A., Fatima, Z., & Hameed, S. (2019). Studies on the antifungal activity of biotemplated gold nanoparticles over Candida albicans. *Materials Research Bulletin, 119*, 110563. https://doi.org/10.1016/j.materresbull.2019.110563
30. Sharma, S., Pal, R., Hameed, S., & Fatima, Z. (2016). Antimycobacterial mechanism of vanillin involves disruption of cell-surface integrity, virulence attributes, and iron homeostasis. *International Journal of Mycobacteriology, 5*(4), 460–468. https://doi.org/10.1016/j.ijmyco.2016.06.010
31. Mosmann, T. (1983). Rapid colorimetric assay for cellular growth and survival: Application to proliferation and cytotoxicity assays. *Journal of lmmunological Methods, 65*(1–2), 55–63. https://doi.org/10.1016/0022-1759(83)90303-4
32. Virmani, I., Sasi, C., Priyadarshini, E., Kumar, R., & Kumar, S. (2020). Comparative anticancer potential of biologically and chemically synthesized gold nanoparticles. *Journal of Cluster Science, 31*(4), 867–876. https://doi.org/10.1007/s10876-019-01695-5
33. Barabadi, H., Webster, T. J., Vahidi, H., Sabori, H., & Damavandi, K. (2020). Green nanotechnology-based gold nanomaterials for hepatic cancer therapeutics: A systematic review, *19*, 3–17. https://doi.org/10.22037/ijpr.2020.113820.14504